Fig.13.

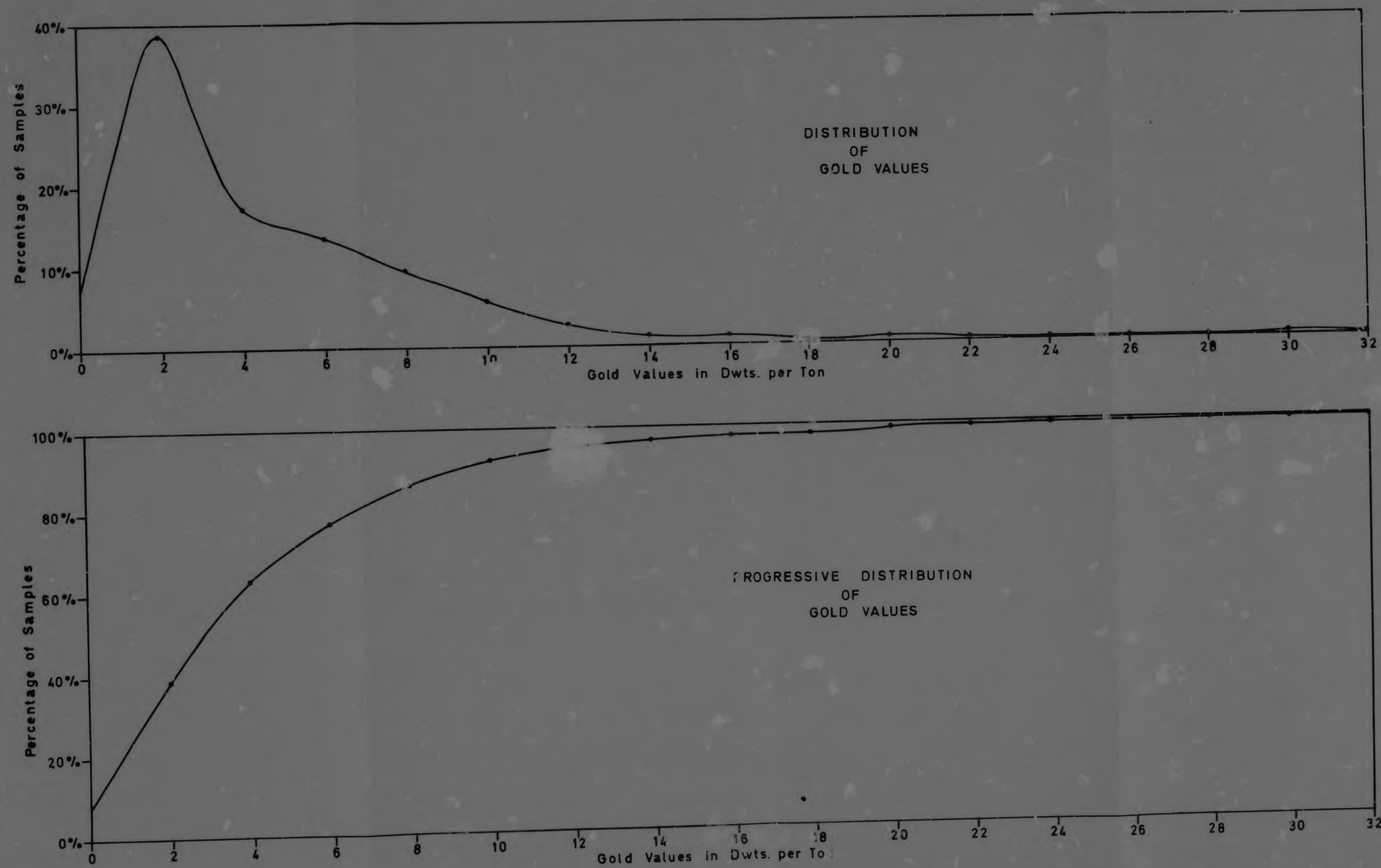
DISTRIBUTION
OF
GOLD VALUES
Percentage of Samples
40%
30%
20%
10%
0%
0
2
4
6
8
10
12
14
16
18
20
22
24
26
28
30
32
Gold Values in Dwts. per Ton
PROGRESSIVE DISTRIBUTION
OF
GOLD VALUES
Percentage of Samples
100%
80%
60%
40%
20%
0%
Gold Values in Dwts. per To

Fig.13.

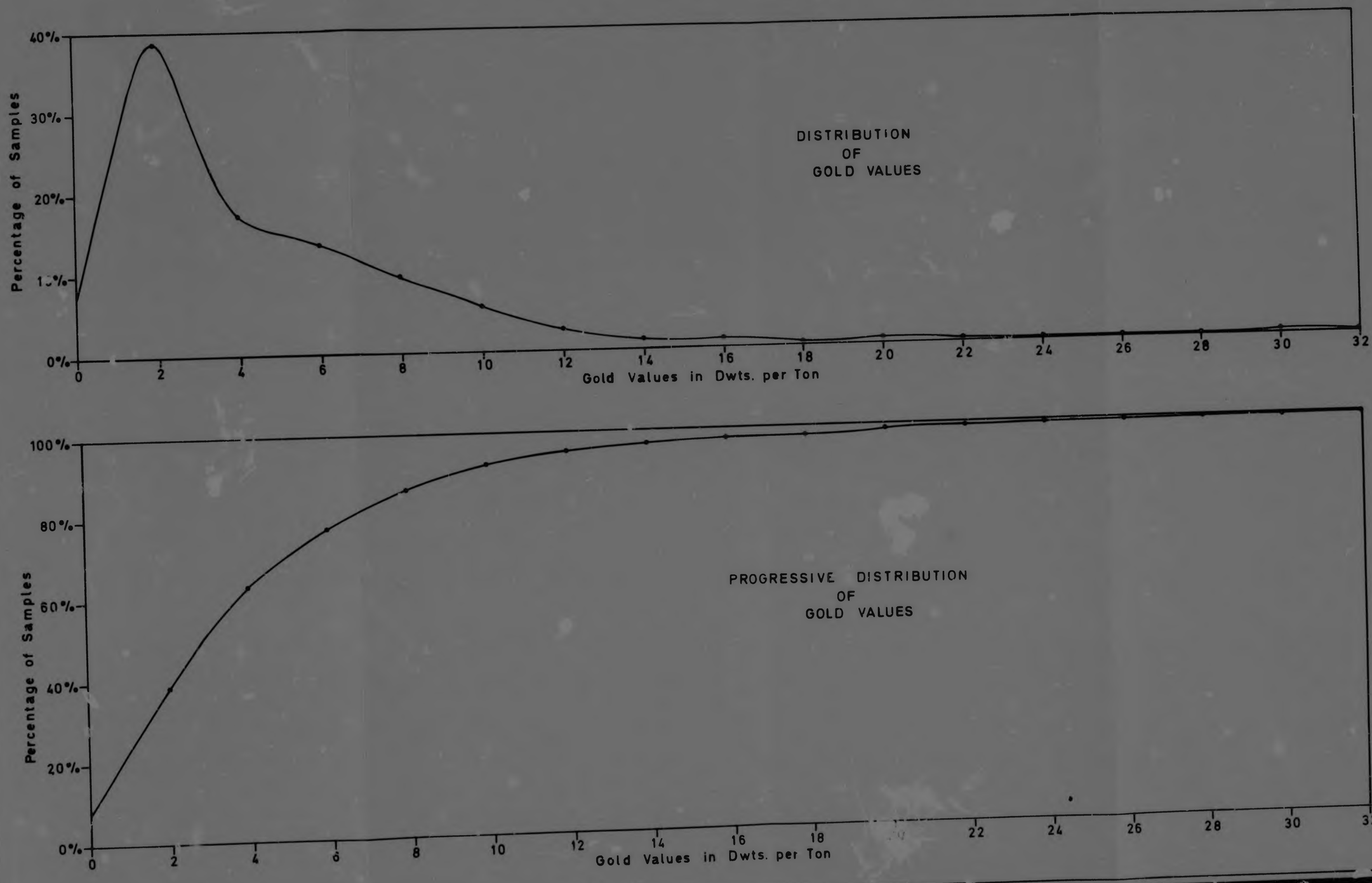
DISTRIBUTION
OF
GOLD VALUES
Percentage of Samples
40%
30%
20%
10%
0%
0
2
4
6
8
10
12
14
16
18
20
22
24
26
28
30
32
Gold Values in Dwts. per Ton
PROGRESSIVE DISTRIBUTION
OF
GOLD VALUES
Percentage of Samples
100%
80%
60%
40%
20%
0%
0
2
4
6
8
10
12
14
16
18
22
24
26
28
30
32
Gold Values in Dwts. per Ton

GRAPH ILLUSTRATING THE RELATIONSHIP OF GOLD SILVER AND IMPURITIES IN BARS OF GOLD BULLION.

Fig.14.

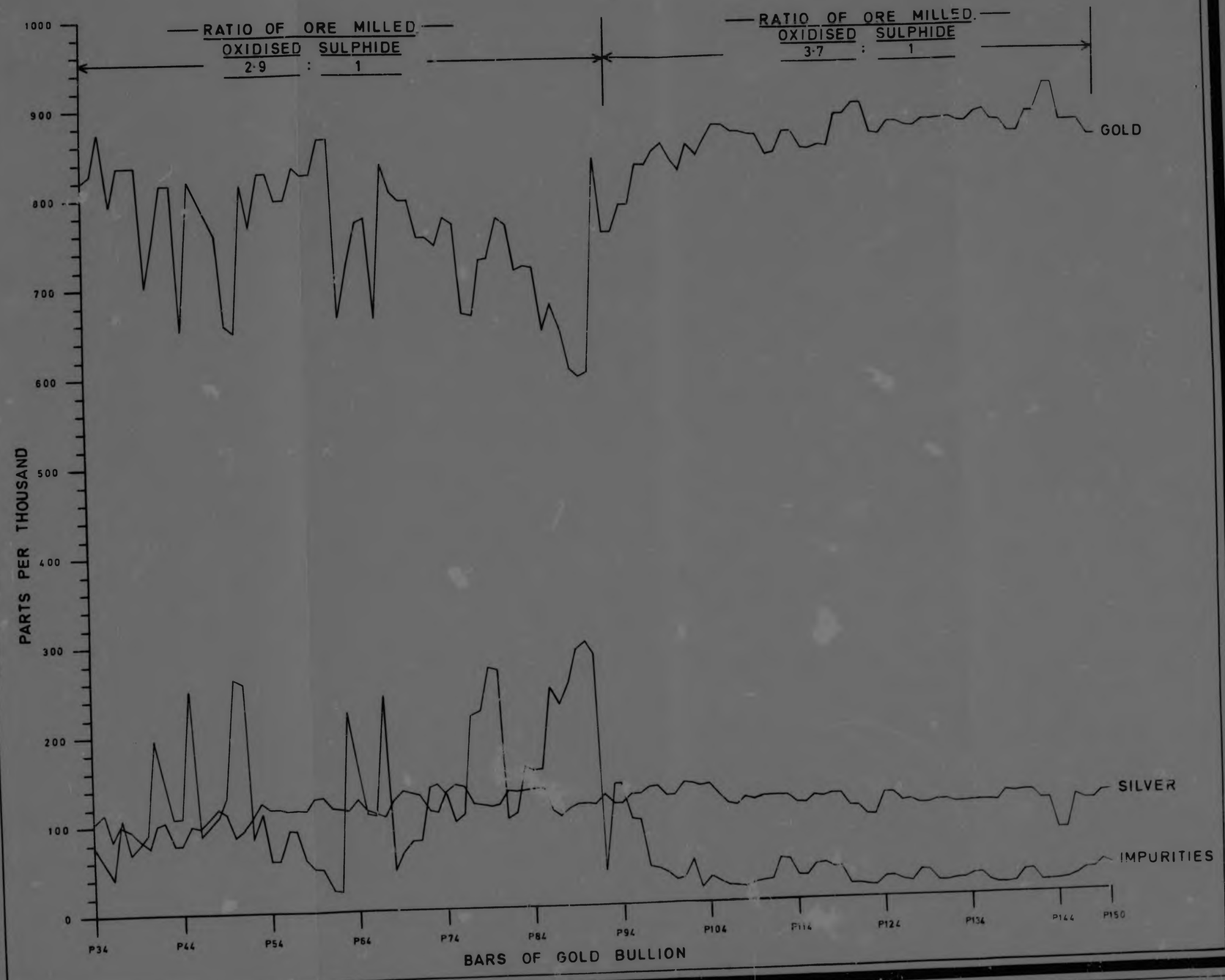

GRAPH ILLUSTRATING THE RELATIONSHIP OF GOLD SILVER AND IMPURITIES IN BARS OF GOLD BULLION.

Fig.15.

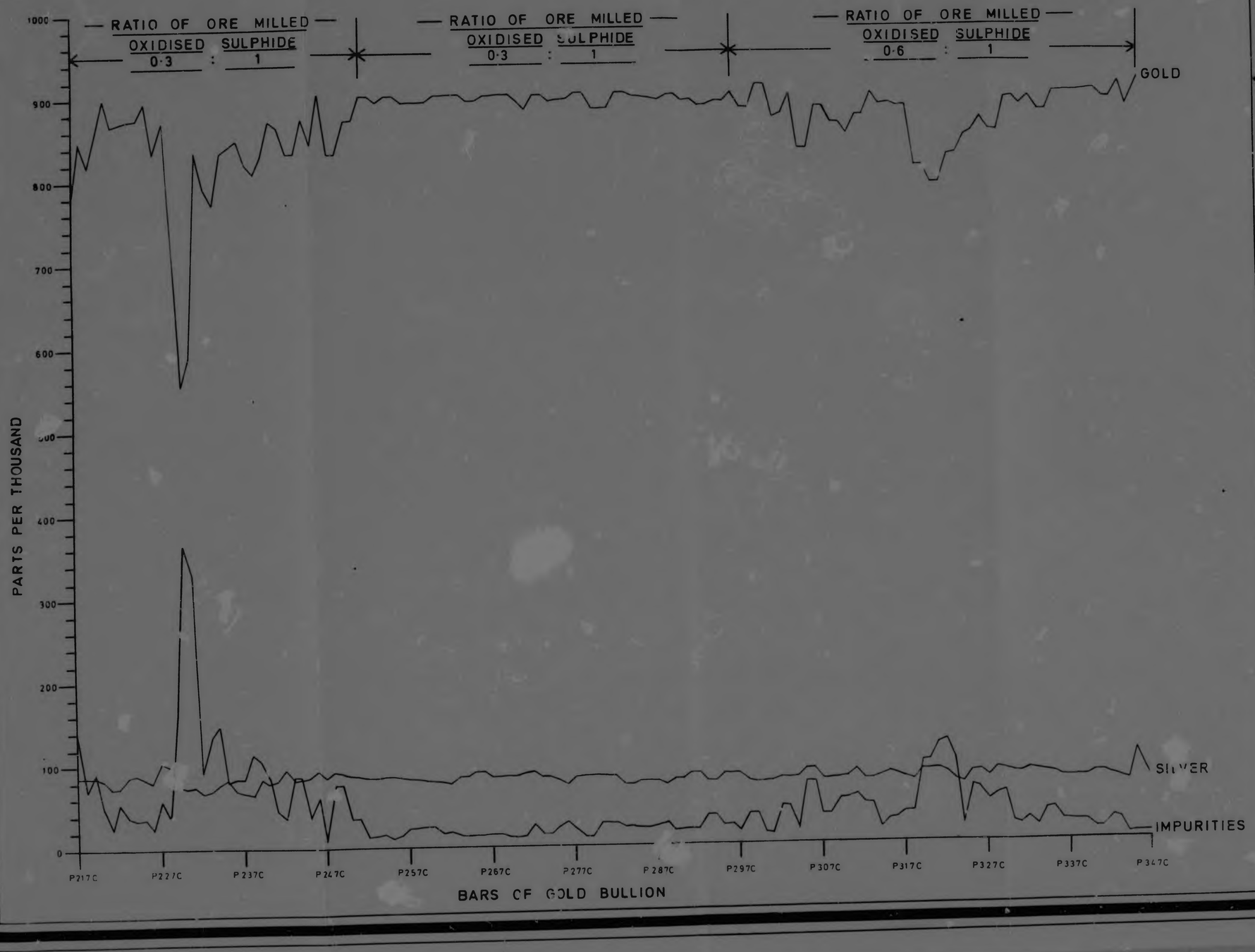

A.

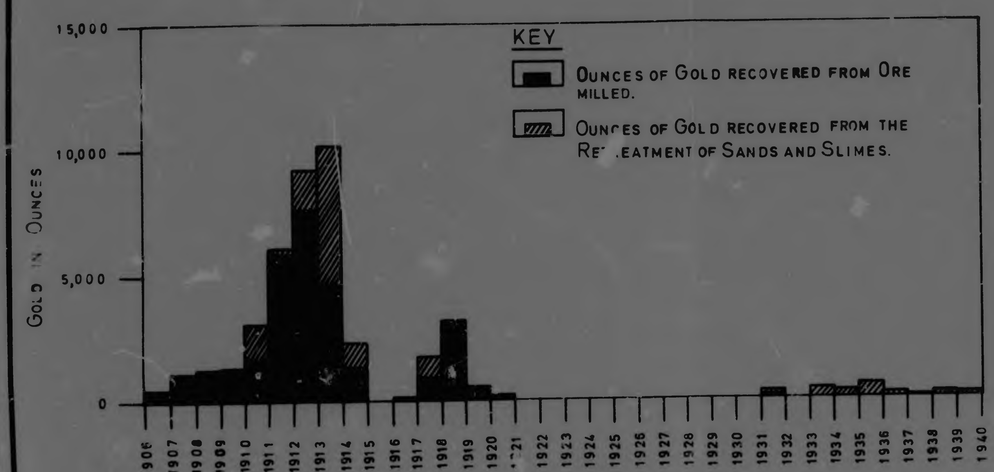

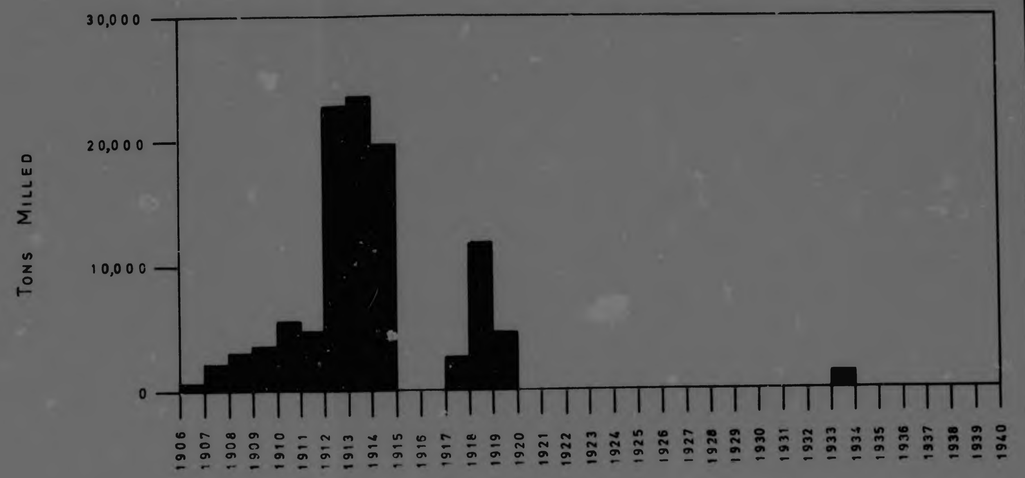

Fig.16.

C.

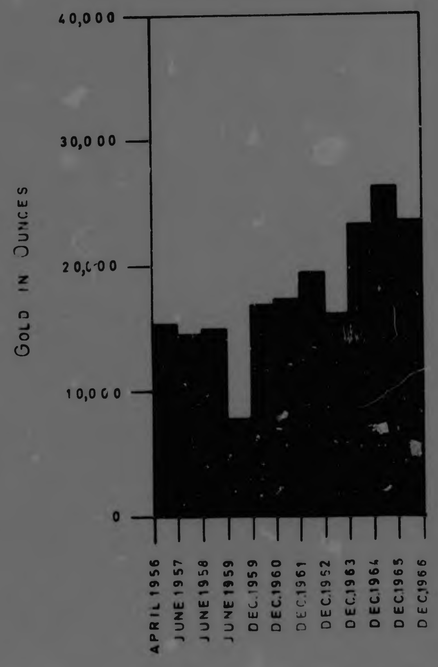

A. HISTOGRAM REPRESENTING OUNCES OF GOLD RECOVERED FOR THE PERIOD 1907 TO 1940.

B. HISTOGRAM REPRESENTING TONS MILLED FOR THE PERIOD 1907 TO 1940.

C. HISTOGRAM REPRESENTING OUNCES OF GOLD RECOVERED FOR THE PERIOD 1956 TO 1966.

D. HISTOGRAM REPRESENTING TONS MILLED FOR THE PERIOD 1956 TO 1966.

D.

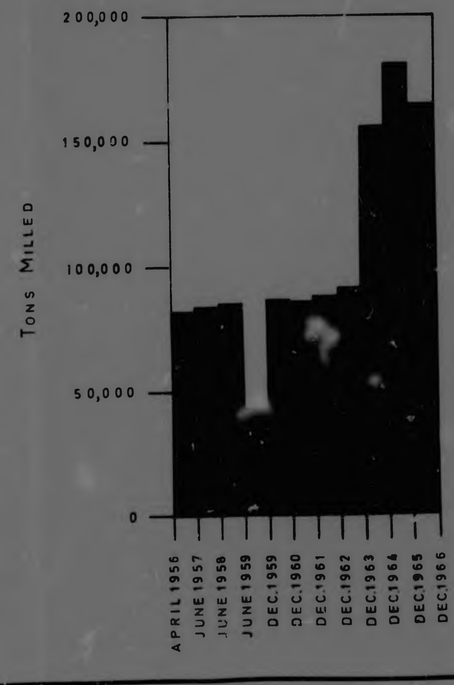

XI. ACKNOWLEDGEMENTS

The author wishes to express his appreciation to the management of Rio Tinto (Rhodesia) Ltd. for permission to publish this thesis.

For their close co-operation and help the author wishes to thank the following members and former members of the Rio Tinto Group, Dr. J. W. N. Sharpe, Dr. F. L. Collender, Messrs. W. V. Rickards, G. Logan, T. H. Park, P. B. Batty, G. C. Bluett, R. Gersteling, T. Blyth, F. van Tonder, P. Connear, P. Luxat and J. Grabe.

The author gratefully acknowledges the help rendered him by his supervisor Professor E. Mendelssohn, as well as members of staff in the department of geology at the University of the Witwatersrand.

Thanks are due to Miss M. Waghorn, Miss L. Bell and Mrs. K. Fahrbach for the typing of this thesis.

To my wife, Diana, and my parents Dr. and Mrs. R. N. Johnson, my sincerest gratitude for their encouraging and continuous support.

XII. REFERENCES

ANHAEUSSER, C. R., ROERING, C., VILJOEN, M.J., VILJOEN, R. P. (1967) The Barberton Mountain Land: A Model of the Elements and Evolution of an Archean Fold Belt. Inform. Circ. No. 38. Econ. Geol. Res. Unit. Univ. Witwatersrand, Johannesburg. 34 p.

BATEMAN, A. M. (1955) Economic Mineral Deposits, 2nd Ed. Chapman and Hall Ltd., London, p. 94 - 136, p. 303 - 314.

De SITTER, L. U. (1956) Structural Geology, 1st Ed. McGraw-Hall Book Co., Inc., New York, p. 87 - 89, p. 251 - 260, p. 292 - 299, p. 442 - 445.

EMMONS, W. H. (1933) On the Mechanism of the Deposition of certain Metalliferous Lode Systems associated with Granitic Batholiths. Lindgren Volume. Amer. Inst. Mining and Metallurgical Engineers, New York, p. 327 - 349

GOVETT, G. J. (1966) Origin of Banded Iron Formations. Geol. Soc. America, Vol. 77, No. 11, p. 1191 - 1206.

HARKER, A. (1956) Metamorphism. Methuen and Co. Ltd., London, p. 177 - 189, p. 203 - 214, p. 277 - 287, p. 344 - 352.

HOLMES, A. (1965) Principles of Physical Geology. New and Fully Revised Edition. Thomas Nelson and Son, Ltd., London, p. 202 - 206, p. 236 - 239, p. 279 - 284 p. 1169 - 1171, p. 1184 - 1186.

KING, L. C. (1962) M[illegible]logy of the Earth. Oli[illegible]r and Boyd, Edinburgh and London, p. 254 - p. 276.

LABERGE, G. L. (1966) Altered Pyroclastic Rocks in Iron-Formation in the Hammersley Range, Western Australia. Econ. Geol. Bull. Soc. Econ. Geologists, Vol. 61, p. 147 - 161.

LABERGE, G. L. (1966) Altered Pyroclastic Rocks in South African Iron-Formation. Econ. Geol. Bull. Soc. Econ. Geologists, Vol. 61, p. 572 - 581.

LEPP, H., GOLDWICH, S. S. (1964) Origin of Precambrian Iron Formations. Econ. Geol. Bull. Soc. Econ. Geologists, Vol. 59, p. 1025 - 1060.

LIGHTFOOT, B. (1934) The Larger Gold Mines of Southern Rhodesia. Geol. Sur. S. Rhod. Bull. No. 26, p. 79 - 80.

MacGREGOR, M. A. (1932) The Geology of the Country around Que Que, Gwelo District. Geol. Sur. S. Rhod. Bull. No. 20, p. 15 - 46.

PETTIJOHN, F. J. (1957) Sedimentary Rocks, 2nd Ed. Harper and Brothers, New York, p. 458 - 464.

PFLUG, H. D. (1966) Structured Organic Remains from the Fig Tree Series of the Barberton Mountain Land. Inform. Circ. No.28, Econ. Geol. Res. Unit,

Univ. Witwatersrand, Johannesburg. 11 p.

RAMBERG, H. (1955) Natural and Experimental Boudinage and Pinch-and-Swell Structures. Jour. Geol. Vol. 63, p. 512-526.

SWIFT, W.H. (1961) An Outline of the Geology of Southern Rhodesia. Geol. Sur. S. Rhod. Bull. No. 50, p. 4 - 17.

WILES, J.W. (1957) The Geology of the Eastern Portion of the Hartley Gold-Belt. Geol. Sur. S.Rhod. Bull. No. 44, Part I, 103 p.

WILES, J.W. (1957) Gold Deposits and Mines. Geol. Sur. S. Rhod. Bull. No. 44, Part II, p. 1 - 4, p. 119 - 122.

ZEALLEY, A. E., LIGHTFOOT, B. (1918) The Geology of the Country around Gatooma. Geol. Sur. S. Rhod. Bull. No. 5, 68 p.

PLATE I

Fig. 1. An aerial photograph of the Pickstone Mine.
Scale:- 1:25,000. Photographed in June, 1966.

Fig. 2. Pickstone Mine plant and the slimes, and flotation tailings dams. Mombi River transgressing lower group of Shamvaian grits, the Pickstone oblique-dip fault, and low, even country of undifferentiated sediments of the upper group of the Shamvaian System.

Fig. 3. Burnett Shaft headgear with rough ore-bin situated behind the compressor water-cooling tank.

Fig. 4. Low, mature, terrain of the Rhodesdale Granite batholith, and peripheral gold-belt rocks of higher relief. Photograph taken from the top of Duchess Hill looking towards the southwest.

Fig. 5. Weathered slabs of highly sheared and foliated felsite and quartz-porphyry. These rocks form the south wall-rock of the Pickstone banded jaspilite host rock.

Fig. 6. Steeply-dipping contact between sheared pillow lava of the Bulawayan System and grits of the Shamvaian System, exposed in the dry bed of the Mombi River.

Fig. 7. High ridge of Shamvaian grits and a lower parallel ridge of Peerless limestone, outcropping behind the Pickstone airfield.

Fig. 8. Old surface workings of the Pickstone banded jaspilite host rock on Concession Hill.

Fig. 9. An ore specimen showing two parallel, milky vein-quartz fracture fillings, obliquely transgressing parallel sulphide-replaced siderite and chert bands. The length of this ore specimen is 14 inches.

Fig. 12. Granite stock. Irregular grains of epidote surrounded by green biotite flakes.
X 30
Open Nicols

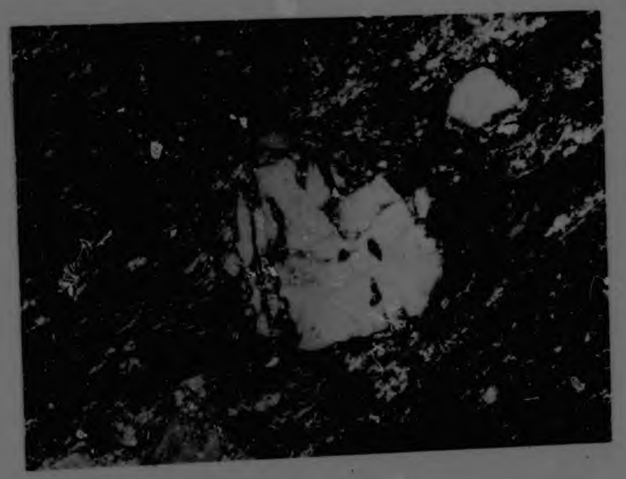

Fig. 13. Speckled chlorite schist, Bulawayan System. Abundant chlorite surrounding a crushed felspar crystal, which is partially sericitized, and beginning to be rolled out to form sericitic lenticules parallel to the schistosity.
X 70
X - Nicols

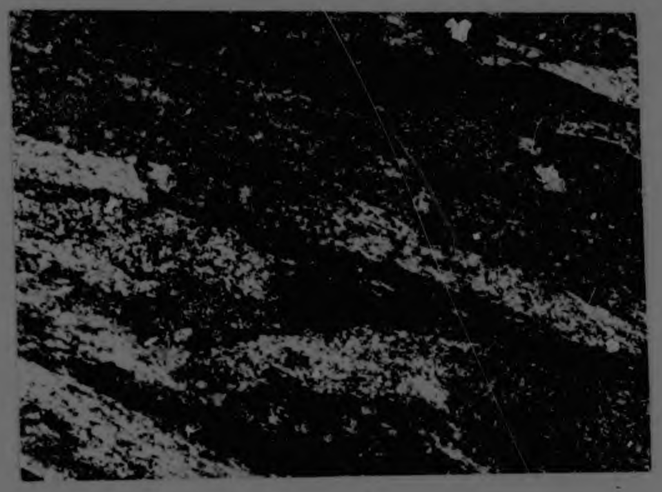

Fig. 14. Speckled chlorite schist, Bulawayan System. Complete sericitization of felspars giving sericitic and chlorite lenticules.

X 70

X - Nicols

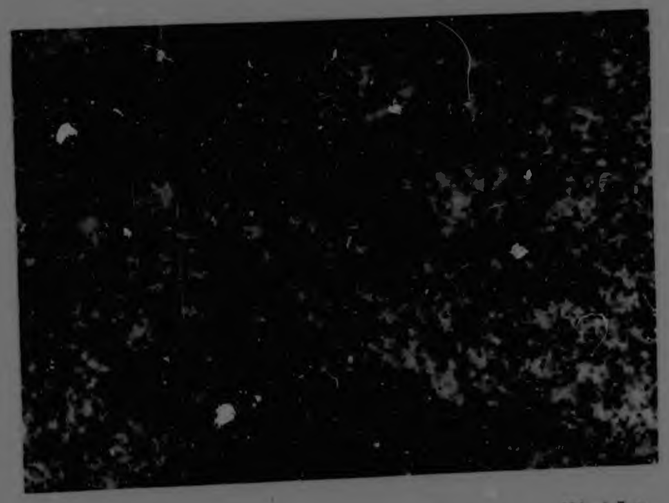

Fig. 15. Felsite extrusive, Bulawayan System. Highly birefringent cryptocrystalline pyrophyllite formed by recrystallization of original felsite constituents.

X 300

X - Nicols

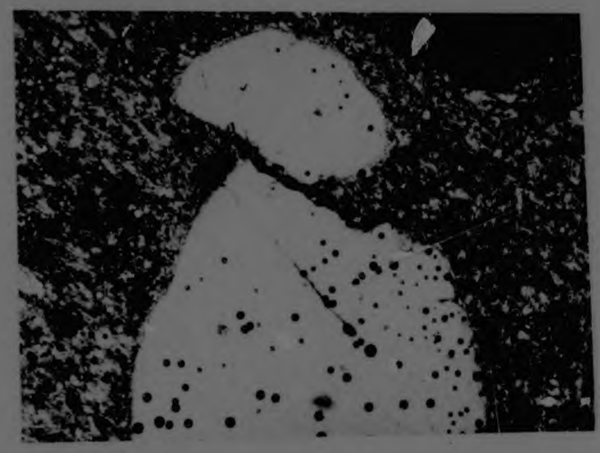

Fig. 16. Quartz-Porphyry, Bulawayan System. Sheared and cracked quartz phenocryst in a crypto-crystalline groundmass of pyrophyllite and quartz.

X 30
X - Nicols

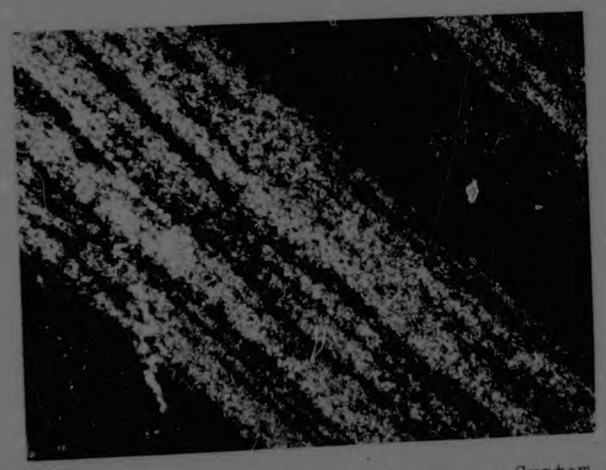

Fig. 17. Banded jaspilite host rock, Bulawayan System. Parallel bands of dark microcrystalline siderite and cryptocrystalline quartz.

X 30
X - Nicols

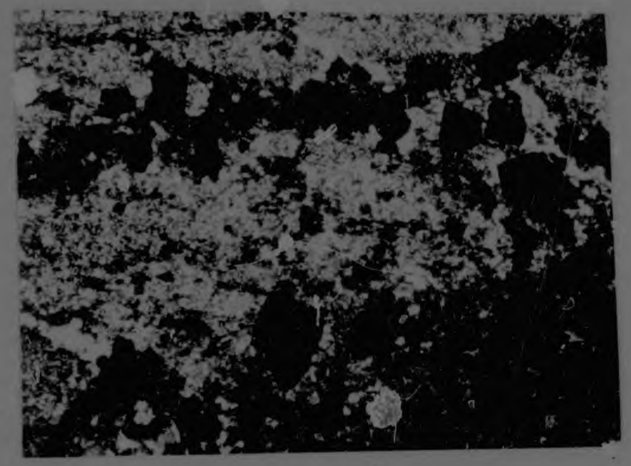

Fig. 18. Banded jaspilite host rock, Bulawayan System. Euhedral and subhedral crystals of arsenopyrite and pyrite, showing preferential replacement of the chemically favourable siderite bands.

X 30
X - Nicols

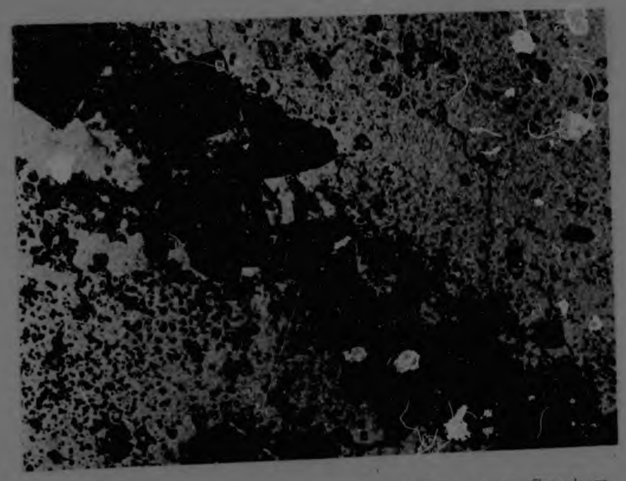

Fig. 19. Banded jaspilite host rock, Bulawayan System. Euhedral and subhedral crystals of arsenopyrite and pyrite replacing siderite band. A few minute rhombohedral crystals of siderite are present.

X 70
X - Nicols

Fig. 20. Banded jaspilite host rock, Bulawayan System. Sulphide crystals surrounded by impressive looking "flame quartz", derived from the recrystallization of the cryptocrystalline quartz.

X 70
X - Nicols

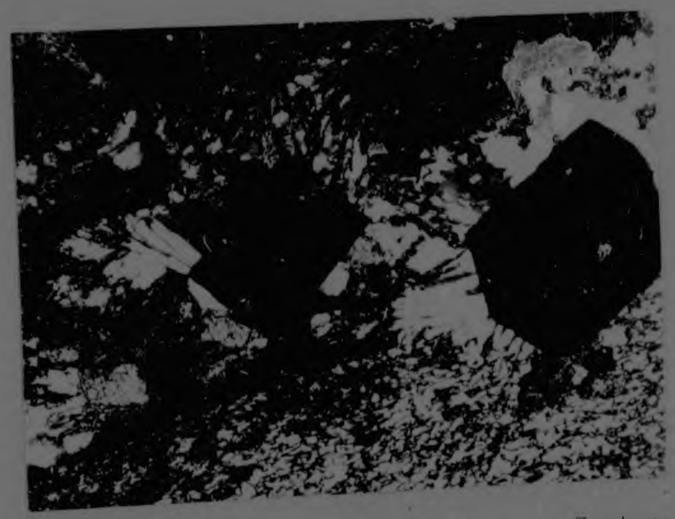

Fig. 21. Banded jaspilite host rock, Bulawayan System. Sulphide crystals replacing siderite and adjacent quartz.

X 70
X - Nicols

Fig. 22. Pillow lava, Bulawayan System. Minute laths of soda-rich plagioclase in a groundmass of chlorite. Small vein filled by highly birefringent carbonate.

X 70
X - Nicols

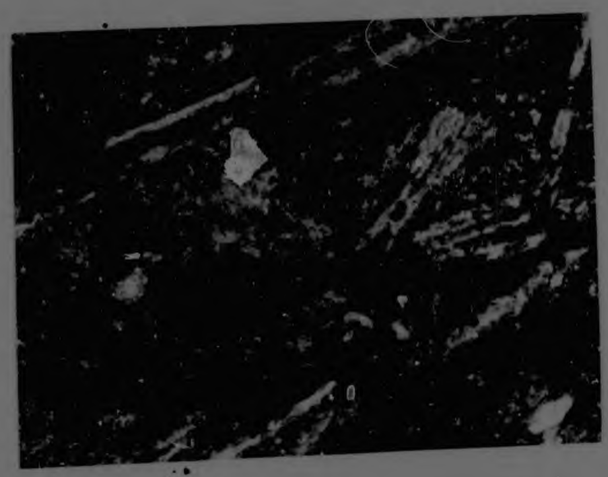

Fig. 23. Pillow lava, Bulawayan System. Twinning in minute laths of plagioclase in a groundmass of chlorite.

X 300
X - Nicols

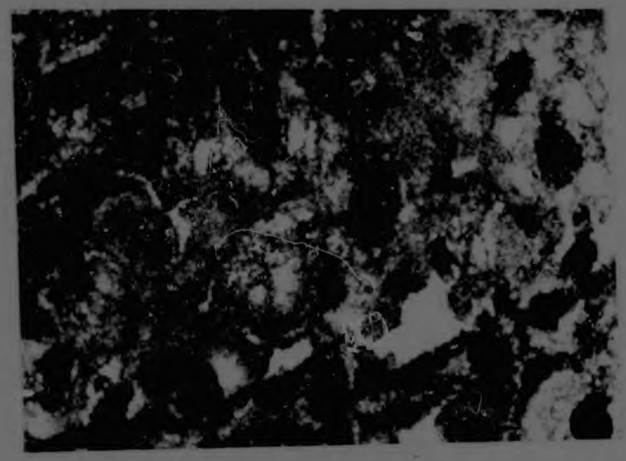

Fig. 24. Pillow lava, Bulawayan System. Microtexture resembling an amygdale and consisting of brown cryptocrystalline unidentifiable material.
X 70
X - Nicols

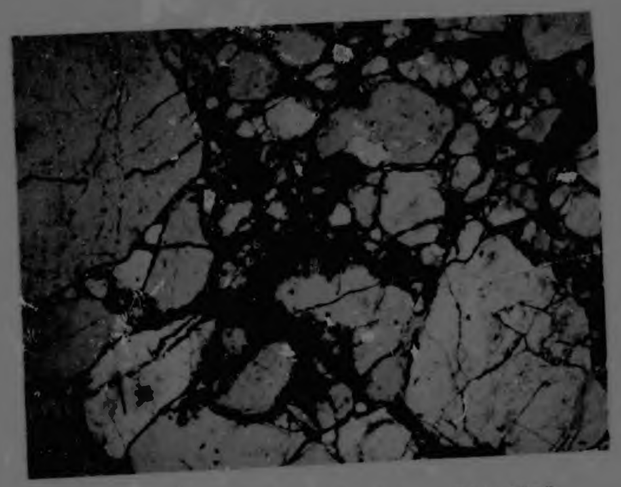

Fig. 25. Quartz grit, Shamvaian System. Ditrital angular quartz grains showing fracturing. Authigenic hematite and hydrated iron oxide occurs interstitially and filling the fractures.
X 30
X - Nicols

Fig. 26. Quartz grit, Shamvaian System. Large subangular quartz grains cemented by small interlocking quartz grains. Birefringent sericite is present interstitially.

X 30
X - Nicols

Fig. 27. Dolerite sill, transgresses the Pickstone banded jaspilite. Augite and andesine showing sub-ophitic and radiating texture. Interiors of some of the andesine crystals are sericitized. Magnetite is prominent.

X 30
X - Nicols

Fig. 28. Variety of crystal shapes shown by arsenopyrite.

X 75

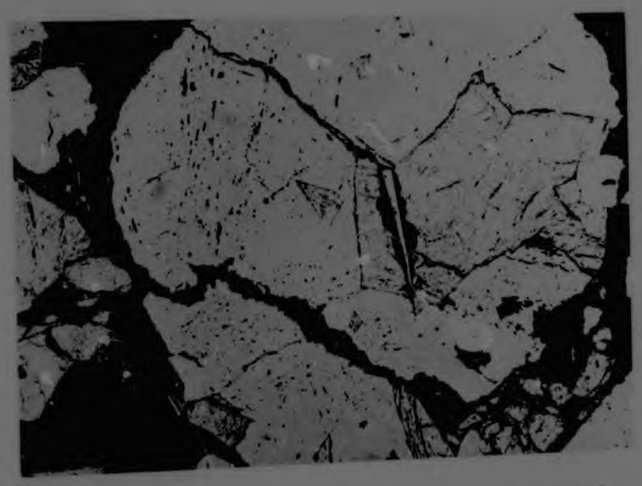

Fig. 29. Subhedral crystals of arsenopyrite (etched) enclosed by massive pitted pyrite.

X 300

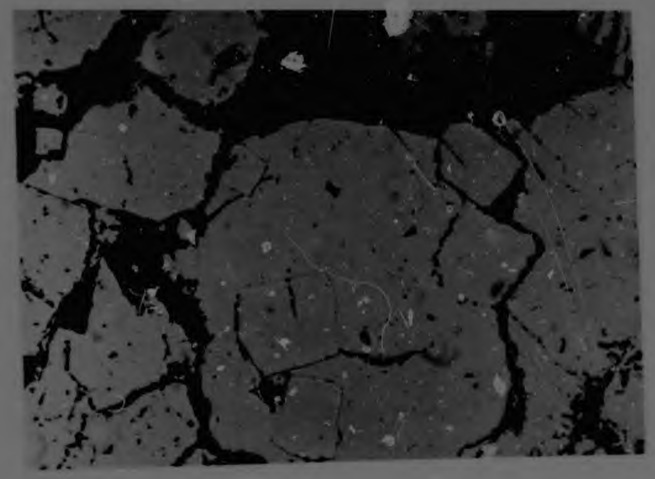

Fig. 30. Pyrite cubes enclosed in massive arsenopyrite.
X 75

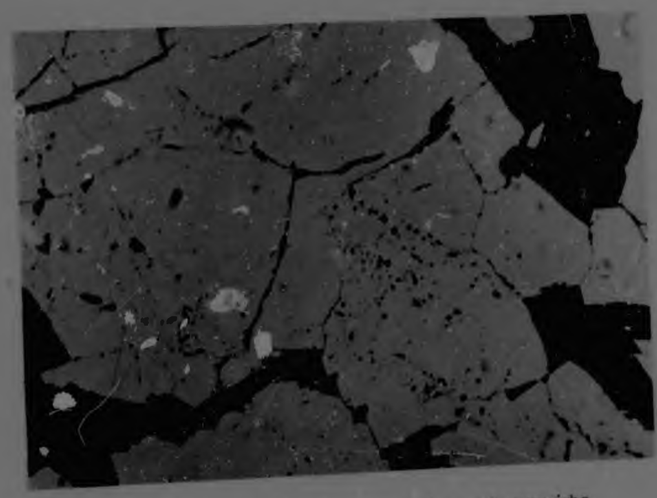

Fig. 31. Interlocking subhedral crystals of pyrite (generally pitted) and arsenopyrite.
X 300

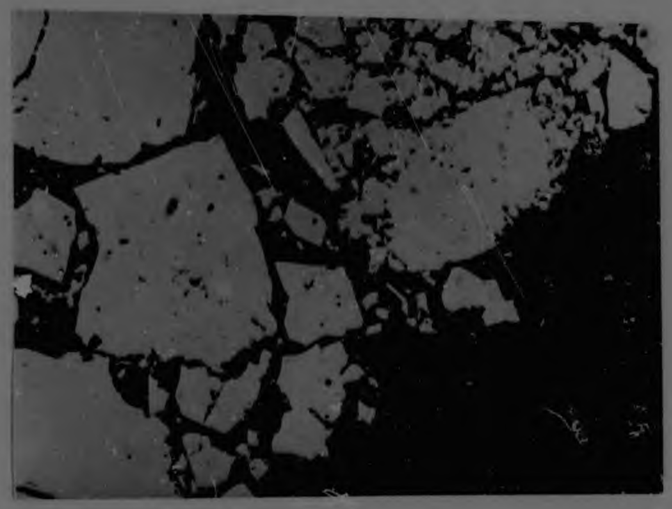

Fig. 32. Fine-grained subhedral crystals of arsenopyrite and pyrite along the boundary of late milky vein-quartz fracture-filling (dark patch) with larger crystals developed further from the vein-quartz.
X 150

Fig. 33. Chalcopyrite (light grey) formed between interlocking grains of arsenopyrite.
X 600

PLATE XVIII

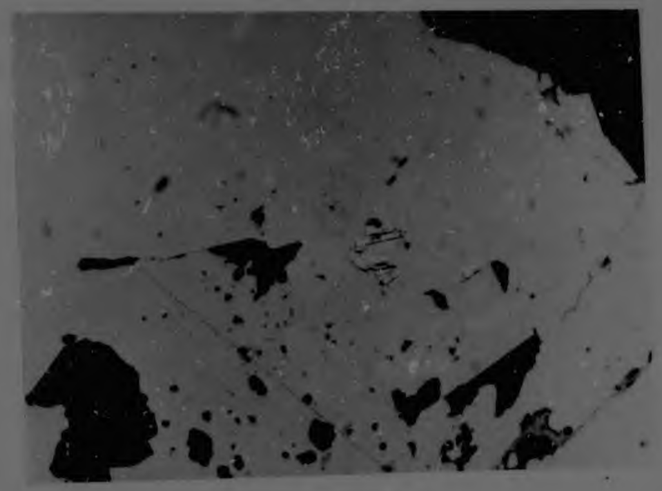

Fig. 34. Gold (scratched) enclosed in arsenopyrite. Chalcopyrite (light grey) filling fractures in the arsenopyrite.

X 300

Fig. 35. Gold (white) between crystals of arsenopyrite and as thin veins filling cracks in the arsenopyrite.

X 600

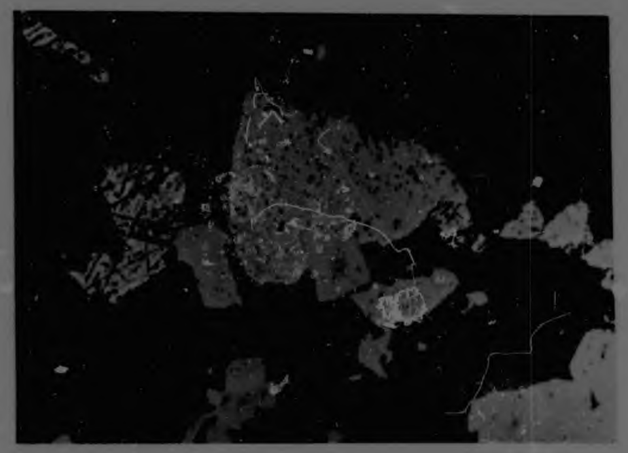

Fig. 36. Gold (scratched) moulded onto subhedral arsenopyrite crystal and massive pitted pyrite.
X 300

Fig. 37. Sphaler te (grey) filling fractures in a crysta. arsenopyrite and as irregular patches along the boundries of the crystal.
X 150

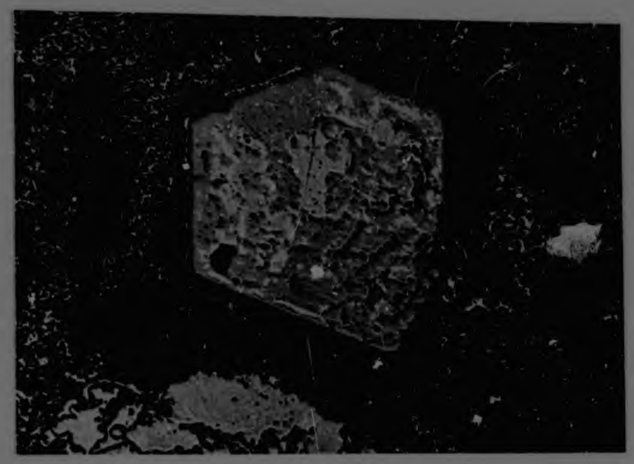

Fig. 38. Pseudomorph of crystal of arsenopyrite altered to hematite and hydrated iron oxide.
X 75